Programmed *in vivo* excision of prophage Φ13 is an essential timing device for the *Staphylococcus aureus* infectious process

Olivier Poupel,[1] Gérald Kenanian,[1] Lhousseine Touqui,[2] Charlotte Abrial,[2] Tarek Msadek[1,6*], Sarah Dubrac[1,3,6*]

[1] Institut Pasteur, Université Paris Cité, CNRS UMR2001, Department of Microbiology, Biology of Gram-Positive Pathogens Unit, F-75015 Paris, France

[2] Institut Pasteur, Université Paris Cité, Department of Global Health, Cystic Fibrosis and Bronchial Diseases Unit, F-75015 Paris, France.

[3] Present address: Institut Pasteur, Université Paris Cité, CNRS UMR6047, Department of Microbiology, Stress Adaptation and Metabolism in Enterobacteria Unit, F-75015 Paris, France

[6]These authors jointly supervised this work : Tarek Msadek, Sarah Dubrac.

*Address correspondence to Tarek Msadek, tmsadek@pasteur.fr, or Sarah Dubrac sarah.dubrac@pasteur.fr

ABSTRACT Mobile genetic elements play an essential part in the infectious process of major pathogens, yet the role of prophage dynamics in *Staphylococcus aureus* remains poorly understood. Here we studied the impact of the Φ13 *hlb*-converting prophage, whose integration inactivates the *hlb* β-toxin gene, on staphylococcal pathogenesis. We showed that prophage Φ13 is lost in approximately half the bacterial population during the course of infection. Inactivation of the Φ13 *int* recombinase gene, essential for insertion/excision, locked the prophage in the bacterial chromosome, leading to a significant loss of virulence in a murine systemic infection model. In contrast, the non-lysogen strain (ΔΦ13), where the *hlb* beta-hemolysin gene is reconstituted, displayed strongly increased virulence. Accordingly, histopathological analyses revealed more severe nephritis in mice infected with bacteria lacking prophage Φ13 (ΔΦ13), in contrast to infection with the parental strain and particularly with the Δ*int* mutant, which led to less severe renal lesions. Cytokine induction in a human neutrophil model showed significantly increased IL-6 expression following infection with the beta-hemolysin producing strain (ΔΦ13). Our results indicate that programmed *in vivo* excision of the Φ13 prophage is essential for progression of the *Staphylococcus aureus* infectious process, since early excision rapidly kills the host whereas the absence of excision significantly lowers staphylococcal virulence.

IMPORTANCE This study highlights prophage Φ13 excision as a critical factor in *S. aureus* pathogenesis, influencing infection outcomes by balancing rapid host killing with reduced bacterial virulence. This mechanism may represent a bet-hedging strategy in genetic regulation, resulting in a mixed bacterial population capable of rapidly switching between two processes: bacterial colonization and host damage. Unraveling this dynamic opens new possibilities for developing targeted therapies to disrupt or modulate prophage activity, offering a novel approach to mitigating *S. aureus* infections.

INTRODUCTION

Staphylococcus aureus, a major human pathogen, causes severe invasive infectious diseases targeting every type of organ, such as pneumonia, endocarditis, osteomyelitis or septicemia. Yet it is also a commensal, asymptomatically colonizing up to 30% of the human population, with the transition between the two lifestyles poorly understood (1). Mobile genetic elements make up approximately 20% of its genome, leading to variations in gene combinations that can strongly influence *S. aureus* virulence (2). Among these, temperate bacteriophages play an important role in genetic variability. Φ13, a member of the Sa3int Siphoviridae *S. aureus* bacteriophage family, is responsible for a dual phenotypic conversion (3, 4) and is by far the most widespread among human clinical isolates (5). Its chromosomal attachment site (*attB*) lies within the coding sequence of the hemolysin B gene, *hlb*, encoding the neutral sphingomyelinase C β-toxin, such that it acts as a phage regulatory switch (6). Φ13 lysogeny leads to disruption of *hlb* and loss of β-hemolytic activity, with excision reconstituting an intact *hlb* gene (5, 7).

Phage Φ13 also carries the *iec* immune evasion cluster including several genes involved in escape from the host innate immune response: *scn*, *chp* and *sak* (8, 9). Natural mobility has been shown for the Φ13-related ΦSa3mw phage in strain MW2 during murine skin colonization and rabbit invasive infection (10, 11).

We studied the effect of phage Φ13 on *S. aureus* virulence during systemic infection. We show that timing of Φ13 prophage excision is essential for pathogenesis, with early β-hemolysin production leading to a strong increase in virulence and elevated levels of the pro-inflammatory cytokine IL-6.

75 **RESULTS**

76

77 **Mobility dynamics of *Staphylococcus aureus* prophages**

78

79 *S. aureus* strain HG001, a derivative of NCTC 8325 (12), carries prophages Φ11, Φ12
80 and Φ13 (7, 13). Specific oligonucleotide primer pairs were designed to detect the
81 presence or absence of each prophage (Supplementary Table 2 and Supplementary Fig.
82 1A). Using chromosomal DNA from a closely related strain cured of all phages,
83 SH1000, an amplicon corresponding to the native bacterial locus without Φ13
84 (oligonucleotide pair OMA7/OMA9, hybridizing on either side of the *attB* site) was
85 detected, but no amplification occurred with oligonucleotides specific for Φ13
86 insertion (OMA7/OMA8) (Supplementary Fig. 1B). With the HG001 Φ13 lysogen
87 strain, both types of amplicon were generated by PCR, suggesting spontaneous Φ13
88 excision within the bacterial population (Supplementary Fig. 1B). We quantified
89 relative prophage levels within the bacterial population by qRT-PCR during growth
90 under optimal laboratory conditions (TSB at 37°C with aeration). Our results indicate
91 that prophage Φ11 is highly mobile with approximately 10% of cells lacking the phage
92 whereas Φ12 was much more stable with less than 0.01% of non-lysogen cells (Fig. 1A).
93 Interestingly, the Φ13 prophage was lost in about 0.5% of the population under these
94 growth conditions (Fig. 1A).

95

96 **Excision of prophage Φ13 is increased *in vivo***

97

98 As shown above, prophage Φ13 is spontaneously excised during growth in laboratory
99 conditions. Since this phage carries genes encoding the SAK staphylokinase virulence
100 factor, as well as SCIN and CHIP, involved in escape from the innate immune response
101 (14), we examined Φ13 excision frequency during the infectious process.
102 We generated a strain carrying the *aad*(9) spectinomycin resistance gene inserted
103 within the Φ13 genome (see Materials and Methods, and Supplementary Table 1 strain
104 ST1387). Four days following sub-lethal (2 x 10^7 c.f.u.) intravenous inoculation with *S.*
105 *aureus* strain ST1387, mice were sacrificed and kidneys collected for c.f.u. counts. Out
106 of 25 harvested kidneys, 18 were colonized by a mixed bacterial population with
107 respect to Φ13 lysogeny (Fig.1B). In some mice a single kidney was colonized with a

108 mixed population with the other only by Φ13 lysogens, suggesting that loss of Φ13 is
109 a *post facto* event to kidney colonization. The average loss of Φ13 was around 50% in
110 the 18 kidneys colonized with a mixed bacterial population (Fig. 1C), a significant
111 increase over the spontaneous excision rate of 0.5% observed during growth *in vitro*.
112 These results suggest that Φ13 excision can be induced and/or the non-lysogen
113 population favored during the infectious process under conditions such as those
114 encountered during kidney colonization.
115
116 **Excision of prophage Φ13 is essential for the *S. aureus* infectious process**
117
118 Increased prophage Φ13 excision during infection suggests it may impact virulence.
119 The Φ13 SAOUHSC-*02293* gene, referred to henceforth as *int*, encodes a protein highly
120 similar to tyrosine recombinase integrases such as Int of phage lambda (13, 15). We
121 deleted the entire coding sequence of the Φ13 *int* gene in *S. aureus* strain HG001 to lock
122 the prophage within the bacterial chromosome. We also constructed a strain where the
123 entire Φ13 genome is deleted, restoring an intact and functional *hlb* gene (see Materials
124 and Methods). These mutations had no effect on bacterial growth *in vitro*
125 (Supplementary Fig. 2). β-hemolytic activity following Φ13 excision was detected on
126 sheep blood agar plates as a distal cold-inducible halo of partial hemolysis (indicated
127 by the white arrow in Fig. 2A).
128 As shown in Fig. 2B, the frequency of Φ13 excision in the Δ*int* mutant is lowered
129 more than 1000-fold as compared to that of the wild type strain (0.6%), confirming the
130 essential role of Int in Φ13 excision. Full complementation of the Δ*int* mutant was
131 obtained by expressing the *int* gene from the Pprot constitutive promoter in the
132 pMK4Pprot-*int* plasmid (Fig. 2B).
133 We next examined the effect on *S. aureus* virulence of either the absence of
134 prophage Φ13 (HG001ΔΦ13 strain, intact *hlb* gene) or the lack of Φ13 excision
135 (HG001Δ*int* strain, *hlb* gene disrupted). As shown in Fig. 3A, using a systemic model
136 of murine infection (5 X 10^7 c.f.u. intravenous injection), the absence of Φ13 with a
137 resulting intact *hlb* gene led to acute virulence with the rapid death of infected animals
138 (50% mortality 24 h post-infection for the ΔΦ13 strain vs. six days for the wild type
139 strain), and more than 90% mortality at the end of the assay (ten days post-infection).
140 Conversely, when Φ13 excision is abolished (Δ*int* strain), *S. aureus* virulence is strongly

141 reduced compared to the wild type strain (31% mortality at the end of the assay, *vs*
142 63%). These results indicate that Φ13 excision and its timing are crucial parameters for
143 the *S. aureus* infectious process.
144
145 **Φ13 dynamics are involved in organ damage during infection**
146
147 To understand the effect of Φ13 dynamics on *S. aureus* virulence, we measured
148 bacterial colonization, and evaluated the kidney lesions of infected mice by
149 histopathological analysis. Mice were inoculated intravenously with sub-lethal
150 concentrations of *S. aureus* cells (approximately 2 X 10^7 c.f.u.). At six days post-infection,
151 mice were sacrificed and one kidney was fixed for histopathological analysis and the
152 other homogenized for c.f.u. counts. Kidney bacterial loads for the parental HG001
153 strain and the HG001ΔΦ13 and HG001Δ*int* mutants were not significantly different
154 (approximately 5 X 10^7 c.f.u. per kidney; Supplementary Fig. 3). However,
155 histopathological analysis revealed nephritis (very probably embolic nephritis) with
156 significantly varying degrees of severity between mice infected with the parental
157 HG001 strain or the ΔΦ13 and Δ*int* mutants. At six days post-infection, mice inoculated
158 with the wild type strain generally displayed mild to moderate nephritis (5/6 mice) or
159 multifocal inflammatory infiltrates (macrophages and other mononucleated cells) in
160 the renal cortex (1/6 mouse) (Fig. 3B1 and 3B2). In contrast, the ΔΦ13 strain leads to
161 more severe nephritis (5/6 mice), with neutrophilic inflammation forming multifocal
162 abscesses, extension to tubules and interstitium, and ischemic necrosis of the papillae
163 (Fig. 3B3 and 3B4). Mice infected with the Δ*int* strain displayed less severe lesions, with
164 mononuclear cell infiltrates mostly in the cortex (4/6 mice) or mild to moderate (1/6
165 mouse) or marked (1/6 mouse) nephritis (Fig. 3B5 and 3B6).
166 These results show that Φ13 dynamics and correlated β-hemolysin production
167 are not essential for host colonization but instead are key factors in host organ damage
168 during infection.
169
170 **Φ13 excision triggers host inflammatory response in infected THP-1 cells**
171
172 Given the major impact of Φ13 excision on virulence and inflammation, we tested its
173 effect on induction of the cellular inflammatory response using human monocytic
174 THP-1 cells. We compared the bacterial internalization capacity of THP-1 cells, the

175 intracellular viability of bacterial cells and the induction of inflammatory markers
176 following infection with the parental HG001 strain and the ΔΦ13 and Δ*int* mutants.
177 THP-1 differentiated macrophages were very efficient for *S. aureus* phagocytosis
178 regardless of prophage content, with nearly 100% of bacteria internalized with a MOI
179 (Multiplicity of Infection) of 10 after 2 hours (Supplementary Fig. 4A). Intracellular
180 survival was not significantly different for the three strains with approximately 10%
181 survival after 24 h post infection and less than 5% after 48 h (Supplementary Fig. 4B).
182 To measure induction of the inflammatory response, duplicate aliquots of infected
183 THP-1 cells were frozen 24 h post-infection, treated to recover cellular RNA and
184 induction of inflammatory cytokine genes measured by qRT-PCR. We measured
185 induction of three pro-inflammatory cytokines previously shown to be induced by
186 *S. aureus* infection, TNFα, IL-1β and IL-6 (16). Although there was no significant
187 difference in induction levels of TNFα and Pro-IL-1β for the three strains, IL-6 gene
188 expression was strongly increased when THP-1 cells were infected with the ΔΦ13
189 strain as compared to the HG001 strain and the Δ*int* mutant (Fig. 4). Thus, lysogeny
190 by Φ13 and the concomitant loss of β-hemolytic activity appear to down-regulate the
191 inflammatory response through lower induction of the pro-inflammatory cytokine IL-
192 6.
193
194 **Impact of *hlb* on *S. aureus* virulence**
195
196 Taken together the results shown above suggest a major role of β-hemolysin
197 production in the increased virulence of the ΔΦ13 strain. To test this hypothesis, we
198 compared the virulence of the ΔΦ13 strain, which produces β-hemolysin, with the
199 virulence of the ΔΦ13Δ*hlb* strain in which the *hlb* gene has also been deleted. As shown
200 in Fig. 5A, 44% of mice infected by the ΔΦ13Δ*hlb* strain survived at nine days post-
201 infection, whereas survival of mice infected by the strain producing β-hemolysin
202 (ΔΦ13) was only 14%, indicating that it is the major factor responsible for the effect of
203 Φ13 excision on *S. aureus* virulence. To test the contribution of Φ13 in virulence, we
204 constructed a strain where both Φ13 and an intact *hlb* gene are present (Δ*int hlb*
205 complemented strain; see Materials and Methods, and Supplementary Table 1). As
206 shown in Fig. 5B, mouse mortality caused by the ΔΦ13 strain producing β-hemolysin
207 but lacking the Φ13 prophage was essentially the same as that following infection by

208 the Δ*int hlb* complemented strain (with both the Φ13 prophage and a functional *hlb*
209 gene). This result confirms the major role of Φ13 dynamics in *S. aureus* virulence by
210 controlling timing of β-hemolysin production during the infectious process.
211

212 **DISCUSSION**

213 *Staphylococcus aureus* is a highly successful human pathogen with a sophisticated
214 arsenal of virulence factors whose production is tightly controlled by multiple
215 regulatory networks, such as two-component systems (17). Further fine-tuning is
216 provided by mobile genetic elements such as pathogenicity islands (SaPI), plasmids,
217 transposons, staphylococcal cassette chromosomes (SCC) and bacteriophages
218 conferring additional virulence factors or antibiotic resistance genes (18). Prophages
219 are widely distributed amongst *S. aureus* strains. Among these, the Φ13 *S. aureus*
220 prophage is inserted within the *hlb* gene encoding β-hemolysin and carries at least
221 three genes involved in host interactions and escape from the immune response,
222 known as the immune evasion cluster (IEC): *sak*, encoding staphylokinase, involved in
223 converting host plasminogen to active plasmin, *scn*, encoding a staphylococcal
224 complement inhibitor, and *chp*, encoding a neutrophil and monocyte chemotaxis
225 inhibitory protein (8). The Φ13 *hlb*-converting prophage family is present in
226 approximately 90% of *S. aureus* clinical isolates (8).

227 β-hemolysin is a sphingomyelinase that can lyse proliferating human
228 lymphocytes, contributing to the host immune evasion (19). Independently of its pore
229 forming activity, β -hemolysin has a biofilm ligase effect by forming a nucleoprotein
230 matrix both in vitro and during infectious endocarditis (20, 21). It has also been shown
231 that Hlb favors mouse skin colonization (11). We noted that *S. aureus* cells isolated
232 from infected mice frequently displayed β-hemolytic activity due to *in vivo* excision of
233 the Φ13 prophage. This prompted us to examine the effect of phage mobility on host
234 pathogen interactions. Our results indicate that mobility of this prophage is required
235 for full virulence of *S. aureus* as part of the time-course of the infectious process. We
236 identified and inactivated the potential integrase gene of this prophage, effectively
237 locking the prophage within the *S. aureus* genome by preventing its excision, and
238 showed that this leads to strongly decreased virulence, with 70% of the mice still
239 surviving after 10 days. Conversely, a strain lacking the Φ13 prophage exhibited
240 greater virulence than the wild type strain, particularly evident in the rapid mortality
241 of infected mice, with 50% succumbing within the first day of infection, compared to
242 six days for the wild-type strain. These Φ13-associated virulence traits are not
243 correlated to differences in the strain's ability to colonize the host, as bacterial loads in
244 the infected kidneys were similar regardless of the strain's lysogenic status. However,

245 kidney damage following infection was strongly associated with the presence of Φ13,
246 showing a clear gradient where a lower proportion of lysogenic bacteria resulted in
247 more severe tissue lesions. In a human monocyte (THP-1) infection model used to
248 assess inflammatory response, we found that the non-lysogenic strain significantly
249 increased the production of the pro-inflammatory cytokine IL-6. IL-6 triggers the
250 release of acute-phase response proteins into the bloodstream, leading to a systemic
251 inflammatory response (22). It is also considered a key biomarker for predicting poor
252 outcomes in sepsis patients and is a promising target for inhibitors to help mitigate the
253 adverse effects of inflammation (16, 23). The induction of IL-6 by the non-lysogenic
254 strain may be linked to its heightened virulence and the significant neutrophil
255 recruitment observed at the inflammation site, as evidenced by the histopathological
256 analysis of infected kidneys.

257 The exact trigger causing excision of Φ13 during infection remains to be
258 established. Interestingly, our observations show that after intravenous infection,
259 kidneys of the same mouse can be colonized differently, one kidney by a lysogenic
260 population, while the other harbors a mixed population. This suggests that Φ13
261 excision is likely induced in the kidneys following colonization rather than during the
262 initial spread of bacteria through the bloodstream. Interestingly, a previous study
263 using a rabbit infection model found that bacteria producing β-hemolysin emerged
264 during organ colonization, but this was not observed in the bacterial population
265 recovered from the bloodstream (10). Stress conditions activating the SOS response are
266 known to induce prophage excision. However, despite many attempts, we were not
267 able to induce Φ13 excision from the bacterial chromosome through treatment with
268 Mitomycin C as SOS-inducing agent. Similar results were previously described with a
269 Newman strain carrying the closely related *hlb*-converting prophage, ΦNM3 (24).
270 More recently, it has been demonstrated that exposure to oxidative stress (such as
271 hydrogen peroxide) and biofilm growth conditions promote the excision of ΦSA3mw
272 (25). This may correlate with our in vivo observations, i.e. that phage induction occurs
273 after organ colonization, under biofilm development conditions.

274 Epidemiological studies have shown that *hlb*-converting prophages are more
275 commonly found in strains colonizing humans (from nasal swabs) than in invasive
276 strains (isolated from blood) (3). Additionally, Φ13-derivative carriers are significantly
277 more frequent in human *S. aureus* strains than in animal strains (26). These *hlb*-
278 converting phages not only inactivate *hlb* but also carry virulence genes, including an

279 immune evasion cluster (IEC) (8). The Sak, SCIN, and CHIPS determinants encoded
280 by this cluster play crucial roles in modulating neutrophil chemotaxis, bacterial
281 phagocytosis, and killing (14). However, their activity is highly specific, primarily
282 targeting the human immune system (27-29). This specificity of the Φ13-derivative IEC
283 in counteracting the human immune response likely contributes to the greater
284 prevalence of *hlb*-converting prophages in human *S. aureus* strains.

285 Interestingly, we demonstrated using an infection mouse model, that the *hlb* gene
286 is the major determinant responsible for the increased virulence observed in the
287 absence of the Φ13 phage. When Hlb is produced, no effect of Φ13 alone was observed
288 (Fig. 5B), likely because the strain is already highly virulent due to constant Hlb
289 production. However, in the absence of *hlb*, the presence of Φ13 led to lowered mouse
290 mortality (Fig. 3A and 5A). While the immune evasion factors encoded by Φ13 have
291 been described as human-specific, it cannot be excluded that they may also exhibit
292 some activity during mouse colonization. Alternatively, Φ13 may encode
293 uncharacterized proteins that could modulate *S. aureus* virulence.

294 Excision of Φ13 and the chromosomal rearrangement reconstituting an intact *hlb*
295 gene can be viewed as a timing device, ensuring that the bacteria first colonize the host,
296 benefiting from the immune evasion cluster proteins encoded by the prophage, with
297 production of β-hemolysin and host tissue damage occurring once the bacteria have
298 reached a threshold level, in agreement with the temporal control of *Staphylococcus*
299 *aureus* virulence factors (30). One of the first examples of prophage excision as a timing
300 device for a developmental process is the *skin* element whose excision leads to a
301 chromosomal rearrangement reconstituting the gene encoding the Sigma K sigma
302 factor, essential for *Bacillus subtilis* sporulation (31, 32).

303 As demonstrated in this study and supported by the literature, the
304 heterogeneity within *S. aureus* populations with respect to *hlb*-converting prophages
305 appears to be a common trait. This could be seen as a bet-hedging strategy, allowing
306 the bacteria to retain the ability to produce both immune evasion proteins (in the
307 lysogenic population) and the potent Hlb cytotoxin (in the non-lysogenic cells).
308 Additionally, since both β-hemolysin and the immune evasion cluster proteins
309 encoded by the prophage are secreted, it is plausible that functional complementation
310 may occur within a mixed population of lysogenic and non-lysogenic bacteria. Similar
311 dual strategies have been observed before, where bistability leads to cell-to-cell
312 variation in gene expression (33, 34). This mixed population with distinct genetic

content would be well-equipped both to resist host defenses during colonization and to cause cellular damage.

316 **MATERIALS AND METHODS**

317 **Bacterial strains and growth media**

318

319 *Escherichia coli* K12 strain DH5α™ (Invitrogen) was used for cloning experiments.
320 *Staphylococcus aureus* strain HG001, derived from strain NCTC 8325 by repairing the
321 mutated *rsbU* gene (12), was used for genetic and functional studies. Plasmids were
322 first transformed into the restriction deficient *S. aureus* strain RN4220 before
323 introduction into the HG001 or derivative strains. *E. coli* strains were grown in LB
324 medium with ampicillin (100 μg/mL) added when required. *S. aureus* strains and
325 plasmids used in this study are listed in Supplementary Table 1. *S. aureus* strains were
326 grown in Trypticase Soy Broth (TSB; Difco) supplemented with chloramphenicol (10
327 μg/mL) or erythromycin (1 μg/mL) when required. *E. coli* and *S. aureus* strains were
328 transformed by electroporation using standard protocols (35) and transformants were
329 selected on LB or Trypticase Soy Agar (TSA; Difco) plates, respectively, with the
330 appropriate antibiotics.

331

332 **DNA manipulations**

333

334 Oligonucleotides used in this study were synthesized by Eurofins Genomics and are
335 listed in Supplementary Table 2. *S. aureus* chromosomal DNA was isolated using the
336 MasterPure™ Gram-positive DNA purification Kit (Epicentre Biotechnologies).
337 Plasmid DNA was isolated using a QIAprep Spin Miniprep kit (Qiagen) and PCR
338 fragments were purified using the Qiaquick PCR purification kit (Qiagen). T4 DNA
339 ligase and restriction enzymes, PCR reagents and Q5 high-fidelity DNA polymerase
340 (New England Biolabs) were used according to the manufacturer's recommendations.
341 Nucleotide sequencing of plasmid constructs was carried out by Eurofins Genomics .

342

343 **Plasmids and mutant strain construction**

344

345 Construction of the ΔΦ13 mutant strain was carried out by cloning an 1800 bp DNA
346 fragment centered around the *attB* site, generated by PCR using oligonucleotides
347 OSA418 and OSA419 and chromosomal DNA from the SH1000 strain (a NCTC8325-4
348 derivative cured for prophages), between the *Bam*HI and *Eco*RI sites of the pMAD
349 vector (36), to give plasmid pMAD-Φ13. For deletion of the Φ13 integrase (*int*; *saouhsc-*

350 *02239*), DNA fragments corresponding to the *int* upstream and downstream regions
351 were generated using oligonucleotides OSA411/OSA412 (900 bp) and
352 OSA413/OSA414 (820 bp) cloned between the pMAD *Bam*HI and *Nco*I sites. The *aad*(9)
353 spectinomycin resistance gene (37) was inserted in the center of the 23 nt intergenic
354 region between the convergent Φ13 *saouhsc-02232* and *saouhsc-02233* genes, to avoid
355 any polar effects on transcription. DNA fragments corresponding to the regions
356 upstream and downstream from the insertion site were generated by PCR using
357 primers OSA508/OSA509 and OSA510/OSA511, respectively, and for the *aad*(9)
358 cassette primers OSA299/OSA470 and plasmid pIC333 (38) as the DNA matrix. The
359 DNA fragments were cloned into pMAD using the *Bam*HI/*Sal*I sites for the upstream
360 fragment, *Sal*I/*Nco*I for the *aad*(9) cassette, and the *Nco*I/*Bgl*II sites for the downstream
361 fragment, generating plasmid pMAD-Φ13*aad*(9). For deletion of *hlb*, we generated
362 upstream and downstream fragments by PCR using oligonucleotides
363 OSA442/OSA443 (884 bp) and OSA444/OSA445 (889 bp) respectively. These
364 fragments were introduced into pMAD between the *Bam*HI and *Eco*RI sites, thus
365 generating the pMAD-*hlb* plasmid. To introduce a functional *hlb* allele into the Φ13
366 lysogenic strain, a pMAD-*hlb*comp plasmid was constructed to place the intact *hlb* gene
367 upstream from the Φ13 genome. A PCR fragment including the *hlb* upstream region
368 and the *hlb* intact gene (1760 bp) was generated using the OSA418 and OSA573 primers
369 and the SH1000 genomic DNA as matrix and it was cloned into pMAD using the
370 *BamH*I and *Sal*I restriction sites. A second PCR fragment corresponding to the part of
371 Φ13 adjacent to *att*L was generated with the OSA574-575 primers and cloned between
372 the *Sal*I and *Bgl*II restriction sites of pMAD.
373 Plasmids were introduced by electroporation into *S. aureus* strain RN4220, and
374 transformants selected at 30°C on TSA plates containing erythromycin and 5-bromo-
375 4-chloro-3-indolyl-β-D-galactopyranoside (X-Gal) (100 μg/mL). Plasmids were then
376 introduced into strain HG001 and integration and excision performed as previously
377 described (36), yielding strains HG001ΔΦ13, HG001Δ*int*, and HG001Φ13-aad(9) and
378 into strain HG001ΔΦ13 for pMAD-*hlb* and HG001Δ*int* for pMAD-*hlb*comp to give
379 strains HG001Δ*int hlb*comp, HG001ΔΦ13Δ*hlb*.
380 Plasmid pMK4Pprot-*int* was used for complementation of the Δ*int* mutant and
381 constructed by cloning the entire *int* coding sequence (amplicon OSA446/OSA447)
382 under the control of the constitutive P*prot* promoter (39).
383

384 **Prophage content measurement by quantitative real time PCRs (qRT-PCRs)**

385

386 Strains were grown overnight in TSB at 37°C, with aeration. Cells were pelleted by
387 centrifugation (2 min, 20,800 *g*) from 2 mL culture samples and genomic DNA
388 extracted using the MasterPure™ Gram Positive DNA Purification Kit (Tebu-Bio).
389 Oligonucleotides were designed with the BEACON Designer 4.02 software
390 (Premier Biosoft International, Palo Alto, CA) to synthesize 100-200 bp amplicons (see
391 Supplementary Table 2). Quantitative real-time PCRs (qRT-PCRs) and critical
392 threshold cycles (CT) were performed and determined using the SsoFast™ EvaGreen
393 Supermix (Bio-Rad, Hercules, CA). All assays were performed using quadruplicate
394 technical replicates, and repeated with three independent biological samples, with one
395 representative experiment shown. Prophage loss frequency was calculated using the
396 formula: $1/(1+2^{\Delta Ct})$ derived from the ΔCt method (40).

397

398 **Hemolysis detection**

399

400 Bacteria were grown overnight in TSB at 37°C with aeration. Culture aliquots (3 µl)
401 were spotted on Columbia plates containing 5% sheep blood (COS, Biomerieux
402 Craponne). Plates were incubated for 24h at 37°C and transferred to 4°C for an
403 additional 24h to for detection of β-hemolysis (41).

404

405 **THP-1 infection experiments**

406

407 THP-1 monocytes were maintained as previously described (42). Differentiation and
408 adherence were obtained by incubation with Phorbol 12-Myristate 13-Acetate (PMA,
409 50 ng/mL) during 4 days at 37°C in a 5%CO_2 atmosphere. Bacterial uptake
410 experiments and survival assays were carried out as previously described (43). Briefly,
411 bacteria were grown in TSB until OD_{600nm} = 1. Cultures were washed in PBS and
412 adjusted to the desired inoculum in RPMI 1640 medium (Gibco), and c.f.u. counts
413 determined by plating serial dilutions on TSA plates. Differentiated THP-1
414 macrophages were incubated with bacteria (MOI = 10) in RPMI 1640 at 37°C with 5%
415 CO2 for 1 h to allow bacterial phagocytosis. They were then washed with RPMI and
416 incubated in RPMI-10% Fetal Calf Serum with streptomycin (100 µg/mL), penicillin
417 (100 U/mL), and gentamycin 40 µg/mL to eliminate extracellular bacteria. At the

418 indicated times, infected macrophages were washed once with RPMI and lysed by
419 incubation in ice-cold water for 15 min and c.f.u. counts were determined by plating
420 serial dilutions on TSA plates. For cytokine gene expression studies by qRT-PCR, THP-
421 1 cells were frozen at -20°C 24h post-infection. Total RNA was extracted using a
422 RNeasy mini kit (Qiagen, CA, USA). Cytokine gene expression was analysed by qRT-
423 PCR using the StepOnePlus real-time PCR system (Applied Biosystems). Primers used
424 for qRT-PCR were TNFα, IL6, pro-IL1beta and HPRT as the reference gene. The qRT-
425 PCRs were performed by Taqman and results presented as relative quantification of
426 gene expression using the $2^{-\Delta\Delta CT}$ method.
427
428 **Animal experiments**
429
430 Seven-week-old female *RjOrl:SWISS* mice (Janvier Labs) were inoculated
431 intravenously with the specified *S. aureus* strains. To analyse Φ13 excision during the
432 infectious process, mice were infected with a sublethal dose (2 x 10^7 c.f.u.) of the Φ13-
433 *aad*(9) strain. Mice were sacrificed four days post-infection and kidneys harvested and
434 homogenized for c.f.u. determination following dilution and plating on TSA and TSA
435 with spectinomycin (100 µg/mL). The rate of prophage excision was calculated as
436 [(c.f.u. on TSA) - (c.f.u. on TSA+spectinomycin)]/(c.f.u. on TSA).
437 Strain HG001 and the Δ*int*, ΔΦ*13*, ΔΦ*13*Δ*hlb* and Δ*int hlb*comp mutants were used
438 for survival studies. Groups of seven mice were injected in the caudal lateral vein with
439 5 X 10^7 c.f.u. per mouse in 0.2 mL. Survival was monitored daily for 9 days following
440 infection and three independent experiments were carried out. To measure kidney
441 colonization and histopathological analysis, mice were infected intravenously with a
442 sublethal dose (1 X 10^7 c.f.u.) of the HG001 parental and Δ*int* and ΔΦ*13* mutant strains
443 (six mice for each strain). At six days post-infection, kidneys were collected and for
444 each mouse, bacterial c.f.u. counts were carried out using one kidney and
445 histopathological observations were done on the other kidney. For histopathology,
446 kidneys were removed and immediately fixed in 10% neutral buffered formalin. After
447 48 h of fixation, the kidneys were longitudinally sectioned through the hilus in order
448 to obtain the renal cortex, medulla, crest, and pelvis on the same section. These
449 samples were embedded in paraffin, and 4-µm sections were cut and stained with
450 hematoxylin and eosin (lesion description) and Gram (bacterial detection).
451

Ethics statement

Animal experiments were carried out at the Institut Pasteur according to European Union guidelines for handling of laboratory animals (http://ec.europa.eu/environment/chemicals/lab_animals/index_en.htm). Animals were monitored daily with a particular attention for any signs of distress. Protocols used were approved by the Institut Pasteur ethics committee (dap160057).

Statistical analysis

Statistical significance in survival experiments was determined using the log-rank, Mantel–Cox test, and significance across means was carried out using *t*-test (GraphPad Prism Software).

ACKNOWLEDGMENTS

We are grateful to Grégory Jouvion for the histopathological analysis, Patrick Trieu-Cuot, in whose lab this work was carried out, and Shaynoor Dramsi for helpful discussion. All authors have read and agreed to the submitted version of the manuscript.

FUNDING

This work was supported by funds from Institut Pasteur, CNRS, and Vaincre La Mucoviscidose Association (Grant «Phage induction, a novel essential factor for *Staphylococcus aureus* infections?»).

AUTHOR CONTRIBUTIONS

Conceptualization: Sarah Dubrac, Lhousseine Touqui, Tarek Msadek.
Data curation: Olivier Poupel, Sarah Dubrac, Lhousseine Touqui, Tarek Msadek.
Formal analysis: Sarah Dubrac, Lhousseine Touqui, Tarek Msadek.
Funding acquisition: Sarah Dubrac, Lhousseine Touqui, Tarek Msadek.
Investigation: Olivier Poupel, Gérard Kénanian, Charlotte Abrial, Sarah Dubrac.
Methodology: Olivier Poupel, Sarah Dubrac.
Project administration: Tarek Msadek, Sarah Dubrac.
Resources: Tarek Msadek, Sarah Dubrac.
Supervision: Tarek Msadek, Sarah Dubrac.
Validation: Tarek Msadek, Sarah Dubrac.
Writing – original draft: Tarek Msadek, Sarah Dubrac.
Writing – review & editing: Tarek Msadek, Sarah Dubrac.

ADDITIONAL FILES

The following material is available online.

Supplemental Material

Supplemental Figures and Tables. Fig. S1–S4 and Tables S1–S2.

501 **REFERENCES**
502

503 1. Piewngam P, Otto M. 2024. *Staphylococcus aureus* colonisation and strategies for
504 decolonisation. Lancet Microbe 5:e606-e618.
505 2. Fitzgerald JR, Sturdevant DE, Mackie SM, Gill SR, Musser JM. 2001.
506 Evolutionary genomics of *Staphylococcus aureus*: insights into the origin of
507 methicillin-resistant strains and the toxic shock syndrome epidemic. Proc. Nat.
508 Acad. Sci. USA: 98:8821-6.
509 3. Goerke C, Pantucek R, Holtfreter S, Schulte B, Zink M, Grumann D, Broker BM,
510 Doskar J, Wolz C. 2009. Diversity of prophages in dominant *Staphylococcus*
511 *aureus* clonal lineages. J. Bacteriol. 191:3462-8.
512 4. Xia G, Wolz C. 2014. Phages of *Staphylococcus aureus* and their impact on host
513 evolution. Infect. Genet. Evol. 21:593-601.
514 5. Goerke C, Wirtz C, Fluckiger U, Wolz C. 2006. Extensive phage dynamics in
515 *Staphylococcus aureus* contributes to adaptation to the human host during
516 infection. Mol. Microbiol.61:1673-85.
517 6. Feiner R, Argov T, Rabinovich L, Sigal N, Borovok I, Herskovits AA. 2015. A
518 new perspective on lysogeny: prophages as active regulatory switches of
519 bacteria. Nat. Rev. Microbiol. 13:641-50.
520 7. Iandolo JJ, Worrell V, Groicher KH, Qian Y, Tian R, Kenton S, Dorman A, Ji H,
521 Lin S, Loh P, Qi S, Zhu H, Roe BA. 2002. Comparative analysis of the genomes
522 of the temperate bacteriophages phi 11, phi 12 and phi 13 of *Staphylococcus*
523 *aureus* 8325. Gene 289:109-18.
524 8. van Wamel WJ, Rooijakkers SH, Ruyken M, van Kessel KP, van Strijp JA. 2006.
525 The innate immune modulators staphylococcal complement inhibitor and
526 chemotaxis inhibitory protein of *Staphylococcus aureus* are located on beta-
527 hemolysin-converting bacteriophages. J. Bacteriol. 188:1310-5.
528 9. Rohmer C, Wolz C. 2021. The role of hlb-converting bacteriophages in
529 *Staphylococcus aureus* host adaption. Microb. Physiol. 31:109-122.
530 10. Salgado-Pabon W, Herrera A, Vu BG, Stach CS, Merriman JA, Spaulding AR,
531 Schlievert PM. 2014. *Staphylococcus aureus* beta-toxin production is common in
532 strains with the beta-toxin gene inactivated by bacteriophage. J. Infect. Dis.
533 146:784-92.
534 11. Katayama Y, Baba T, Sekine M, Fukuda M, Hiramatsu K. 2013. Beta-hemolysin
535 promotes skin colonization by *Staphylococcus aureus*. Journal of Bacteriology
536 195:1194-203.

537 12. Herbert S, Ziebandt AK, Ohlsen K, Schafer T, Hecker M, Albrecht D, Novick R,
538 Gotz F. 2010. Repair of global regulators in *Staphylococcus aureus* 8325 and
539 comparative analysis with other clinical isolates. Infect. Immun. 78:2877-89.
540 13. Gillaspy AF, Worrell V, Orvis J, Roe BA, Dyer DW, Iandolo JJ. 2006. The
541 *Staphylococcus aureus* NCTC 8325 Genome, p 381-412. *In* Fischetti VA, Novick
542 RP, Ferretti JJ, Portnoy DA, Rood JI (ed), Gram-Positive Pathogens, 2nd ed.
543 ASM Press, Washington, DC.
544 14. Rooijakkers SH, van Kessel KP, van Strijp JA. 2005. Staphylococcal innate
545 immune evasion. Trends Microbiol. 13:596-601.
546 15. Nunes-Duby SE, Kwon HJ, Tirumalai RS, Ellenberger T, Landy A. 1998.
547 Similarities and differences among 105 members of the Int family of site-specific
548 recombinases. Nucleic Acids Res. 26:391-406.
549 16. van den Berg S, Laman JD, Boon L, ten Kate MT, de Knegt GJ, Verdijk RM,
550 Verbrugh HA, Nouwen JL, Bakker-Woudenberg IA. 2013. Distinctive cytokines
551 as biomarkers predicting fatal outcome of severe *Staphylococcus aureus*
552 bacteremia in mice. PLoS One 8:e59107.
553 17. Haag AF, Bagnoli F. 2017. The role of two-component signal transduction
554 systems in *Staphylococcus aureus* virulence regulation. Curr. Top. Microbiol.
555 Immunol. 409:145-198.
556 18. Lindsay JA. 2010. Genomic variation and evolution of *Staphylococcus aureus*. Int
557 J. Med. Microbiol. 300:98-103.
558 19. Huseby M, Shi K, Brown CK, Digre J, Mengistu F, Seo KS, Bohach GA,
559 Schlievert PM, Ohlendorf DH, Earhart CA. 2007. Structure and biological
560 activities of beta toxin from *Staphylococcus aureus*. J. Bacteriol. 189:8719-26.
561 20. Herrera A, Vu BG, Stach CS, Merriman JA, Horswill AR, Salgado-Pabon W,
562 Schlievert PM. 2016. *Staphylococcus aureus* beta-toxin mutants are defective in
563 biofilm ligase and sphingomyelinase activity, and causation of infective
564 endocarditis and sepsis. Biochemistry 55:2510-7.
565 21. Huseby MJ, Kruse AC, Digre J, Kohler PL, Vocke JA, Mann EE, Bayles KW,
566 Bohach GA, Schlievert PM, Ohlendorf DH, Earhart CA. 2010. Beta toxin
567 catalyzes formation of nucleoprotein matrix in staphylococcal biofilms. Proc.
568 Nat. Acad. Sci. USA: 107:14407-12.
569 22. Tanaka T, Narazaki M, Kishimoto T. 2014. IL-6 in inflammation, immunity, and
570 disease. Cold Spring Harb. Perspect. Biol. 6:a016295.

571 23. Cao YZ, Tu YY, Chen X, Wang BL, Zhong YX, Liu MH. 2012. Protective effect
572 of Ulinastatin against murine models of sepsis: inhibition of TNF-alpha and IL-
573 6 and augmentation of IL-10 and IL-13. Exp. Toxicol. Pathol. 64:543-7.
574 24. Bae T, Baba T, Hiramatsu K, Schneewind O. 2006. Prophages of *Staphylococcus*
575 *aureus* Newman and their contribution to virulence. Mol. Microbiol. 62:1035-47.
576 25. Tran PM, Feiss M, Kinney KJ, Salgado-Pabon W. 2019. ØSa3mw prophage as a
577 molecular regulatory switch of *Staphylococcus aureus* β-toxin production. J.
578 Bacteriol. 201:e00766-18
579 26. Verkaik NJ, Benard M, Boelens HA, de Vogel CP, Nouwen JL, Verbrugh HA,
580 Melles DC, van Belkum A, van Wamel WJ. 2011. Immune evasion cluster-
581 positive bacteriophages are highly prevalent among human *Staphylococcus*
582 *aureus* strains, but they are not essential in the first stages of nasal colonization.
583 Clin. Microbiol. Infect. 17:343-8.
584 27. de Haas CJ, Veldkamp KE, Peschel A, Weerkamp F, Van Wamel WJ, Heezius
585 EC, Poppelier MJ, Van Kessel KP, van Strijp JA. 2004. Chemotaxis inhibitory
586 protein of *Staphylococcus aureus*, a bacterial antiinflammatory agent. J. Exp. Med.
587 199:687-95.
588 28. Kwiecinski J, Josefsson E, Mitchell J, Higgins J, Magnusson M, Foster T, Jin T,
589 Bokarewa M. 2010. Activation of plasminogen by staphylokinase reduces the
590 severity of *Staphylococcus aureus* systemic infection. J. Infect. Dis. 202:1041-9.
591 29. Rooijakkers SH, Ruyken M, Roos A, Daha MR, Presanis JS, Sim RB, van Wamel
592 WJ, van Kessel KP, van Strijp JA. 2005. Immune evasion by a staphylococcal
593 complement inhibitor that acts on C3 convertases. Nat. Immunol. 6:920-7.
594 30. Novick RP. 2003. Autoinduction and signal transduction in the regulation of
595 staphylococcal virulence. Mol. Microbiol. 48:1429-49.
596 31. Stragier P, Kunkel B, Kroos L, Losick R. 1989. Chromosomal rearrangement
597 generating a composite gene for a developmental transcription factor. Science
598 243:507-12.
599 32. Kunkel B, Losick R, Stragier P. 1990. The *Bacillus subtilis* gene for the
600 development transcription factor sigma K is generated by excision of a
601 dispensable DNA element containing a sporulation recombinase gene. Genes
602 Dev. 4:525-35.
603 33. Dubnau D, Losick R. 2006. Bistability in bacteria. Mol. Microbiol. 61:564-72.
604 34. Veening JW, Smits WK, Kuipers OP. 2008. Bistability, epigenetics, and bet-
605 hedging in bacteria. Annu. Rev. Microbiol. 62:193-210.

606 35. Sambrook J, Fritsch EF, Maniatis T. 1989. Molecular cloning : a laboratory
607 manual, second edition. Cold Spring Harbor Laboratory, Cold Spring Harbor,
608 N. Y.
609 36. Arnaud M, Chastanet A, Debarbouille M. 2004. New vector for efficient allelic
610 replacement in naturally nontransformable, low-GC-content, gram-positive
611 bacteria. Appl. Environ. Microbiol. 70:6887-91.
612 37. Murphy E. 1985. Nucleotide sequence of a spectinomycin adenyltransferase
613 AAD(9) determinant from *Staphylococcus aureus* and its relationship to AAD(3")
614 (9). Mol. Gen. Genet. 200:33-39.
615 38. Steinmetz M, Richter R. 1994. Easy cloning of mini-Tn*10* insertions from the
616 *Bacillus subtilis* chromosome. J. Bacteriol. 176:1761-3.
617 39. Archambaud C, Gouin E, Pizarro-Cerda J, Cossart P, Dussurget O. 2005.
618 Translation elongation factor EF-Tu is a target for Stp, a serine-threonine
619 phosphatase involved in virulence of *Listeria monocytogenes*. Mol. Microbiol.
620 56:383-96.
621 40. Livak KJ, Schmittgen TD. 2001. Analysis of relative gene expression data using
622 real-time quantitative PCR and the 2(-Delta Delta C(T)) method. Methods
623 25:402-8.
624 41. Haque RU, Baldwin JN. 1964. Types of hemolysins produced by *Staphylococcus*
625 *aureus*, as determined by the replica plating technique. J. Bacteriol. 88:1442-7.
626 42. Stokes RW, Doxsee D. 1999. The receptor-mediated uptake, survival, replication,
627 and drug sensitivity of *Mycobacterium tuberculosis* within the macrophage-like
628 cell line THP-1: a comparison with human monocyte-derived macrophages.
629 Cell. Immunol. 197:1-9.
630 43. Soutourina O, Dubrac S, Poupel O, Msadek T, Martin-Verstraete I. 2010. The
631 pleiotropic CymR regulator of *Staphylococcus aureus* plays an important role in
632 virulence and stress response. PLoS Pathog. 6:e1000894.
633

634 **FIGURE LEGENDS**
635
636 **Figure 1: Prophage Φ13 in vitro and in vivo.** A) Prophage excision frequencies in
637 strain HG001. qRT-PCR quantification of Φ11, 12, and 13 prophage content in *S. aureus*
638 strain HG001 grown in TSB at 37°C with aeration. Specific primer pairs are described
639 in Supplementary Table 2. The results are the mean of 4 technical replicates and are
640 representative of 3 independent biological replicates.
641 B) Quantification of Φ13 lysogens in bacterial populations from infected kidneys. Mice
642 were infected from the caudal lateral vein with a sub-lethal dose (2 X 10^7 c.f.u.) of *S.*
643 *aureus* strain HG001 Φ13::*aad*(9). Mice were sacrificed four days post-infection and
644 kidneys harvested for c.f.u. counts on TSA and TSA with spectinomycin. 25 infected
645 kidneys were examined and the proportion of homogeneous lysogen population (less
646 than 0.5% non-lysogen) and heterogeneous bacterial population with a mix of lysogen
647 and non-lysogen bacteria is shown.
648 C) Proportion of non-lysogen bacteria per kidney in organs infected with a mixed
649 population of lysogenic and non-lysogenic bacteria.
650
651 **Figure 2: Characterization of the *S. aureus* Δ*int* and ΔΦ13 mutants.** Strains were
652 grown overnight at 37°C with aeration. A) 3 µl of the bacterial cultures was spotted on
653 sheep blood agar plates and incubated consecutively for 24 h at 37°C and 24 h at 4°C
654 to detect hemolytic activities. The white arrow indicates the β-hemolytic halo
655 characteristic of bacteria lacking prophage Φ13. B) Prophage Φ13 excision frequency
656 detected by qRT-PCR using oligonucleotide pairs OMA7-OMA8 and OMA7-OMA9
657 specific for the presence or absence of Φ13, respectively. Results are presented as
658 means ± SEM of 3 replicates and *t*-test was used to compare WT and Δ*int* results (***,
659 p<0,0001).
660
661 **Figure 3: Impact of prophage Φ13 and *hlb* on *S. aureus* virulence.** A) Kaplan-Meier
662 survival curves of *RjOrl:SWISS* mice infected intravenously with *S. aureus* HG001 wild
663 type strain and the Δ*int* and ΔΦ13 mutants (5 X 10^7 c.f.u./injection). A total of 14 mice
664 were used in each group in two independent experiments. For each strain, the
665 genotype is indicated followed by the relevant genetic context (presence or absence of
666 prophage Φ13 and a functional *hlb* gene). Statistical analysis of data using Log-rank
667 (Mantel Cox) test was performed to compare each mutant strain to the HG001 parental

668 strain. WT/Δ*int*: *p*=0.0077; WT/ ΔΦ13 : *p*=0.0021. B) Histopathological kidney analyses
669 6 days post-infection by intravenous inoculation with sub-lethal bacterial loads (2 X
670 10^7 c.f.u./injection) of the *S. aureus* HG001 wild type (1 and 2), Δ*int* (3 and 4) and ΔΦ13
671 (5 and 6) strains. Most (5/6) mice infected with the wild type strain displayed mild to
672 moderate nephritis, with neutrophilic infiltrates/abscesses (black arrowheads) of
673 varying sizes in the cortex (1), medulla, and papilla (2). Infection with strain ΔΦ13 led
674 to more severe nephritis (5/6 mice), with multifocal abscesses (3 and 4, black
675 arrowheads), extension to tubules and interstitium, and ischemic necrosis of the
676 papilla (4, black arrow). Most mice (4/6) infected with the Δ*int* strain displayed less
677 severe lesions, with mononuclear cell infiltrates most often in the cortex (5, not seen at
678 a low magnification) but also in the papilla (6, arrowhead).
679
680 **Figure 4: Impact of Φ13 on cytokine induction by THP-1 neutrophils.** PMA-activated
681 THP-1 cells were infected with the HG001 wild type strain or the ΔΦ13 and Δ*int*
682 mutants with a MOI=10. After 24 H of infection, cytokine gene expression was
683 determined by qRT-PCR performed with cDNA synthesized from RNA of THP-1 cells
684 infected by the indicated strains (dark grey) or non-infected control (light grey).
685 Expression levels are given in arbitrary units normalized against that of HPRT. Each
686 experiment was carried out 6 times in two independent series (means ± SD). ***:
687 *P*<0.005 (*t*-test).
688
689 **Figure 5: Impact of *hlb* on *S. aureus* virulence.** Kaplan-Meier survival curves of
690 *RjOrl:SWISS* mice infected intravenously with *S. aureus* HG001 wild type strain and
691 the Δ*int* hlb_{comp}, ΔΦ13 and ΔΦ13Δ*hlb* mutants (5 X 10^7 c.f.u./injection). A total of 14 mice
692 were used in each group in two independent experiments. *, *P*<0.05 and **, *P*<0.01
693 (Wilcoxon test). For each strain, the genotype is indicated followed by the relevant
694 genetic context (presence or absence of prophage Φ13 and a functional *hlb* gene).
695 A) Role of *hlb* in virulence by comparing infection with the HG001 strain and the ΔΦ13
696 and ΔΦ13Δ*hlb* derivatives.). Statistical analysis of data using Log-rank (Mantel Cox)
697 test was performed to compare each mutant strain to the HG001 parental strain.
698 WT/ΔΦ13Δ*hlb*: *p*=0.6157 (ns); WT/ΔΦ13 : *p*=0.0039.
699 B) Role of Φ13 in virulence by comparing infection with the HG001 strain and the
700 Δ*int* hlb_{comp} (dashed line) and ΔΦ13 derivatives. Statistical analysis of data using Log-

701 rank (Mantel Cox) test was performed to compare each mutant strain to the HG001
702 parental strain. WT/Δ*int hlb*$_{comp}$: p=0.0147; WT/ΔΦ13 : p=0.0066.

Figure 1

A.

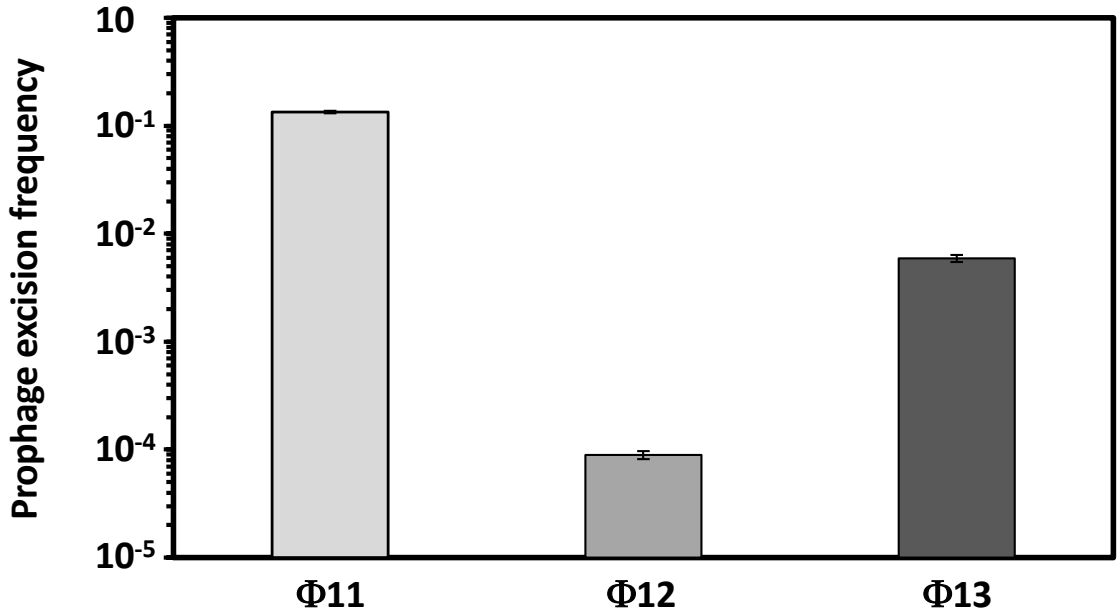
Prophage excision frequency
10
10-1
10-2
10-3
10-4
10-5
Φ11
Φ12
Φ13

B.

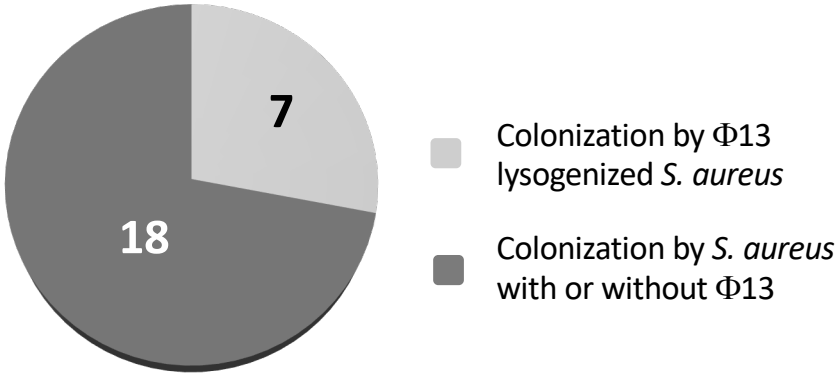
7
18
Colonization by Φ13 lysogenized *S. aureus*
Colonization by *S. aureus* with or without Φ13

C.

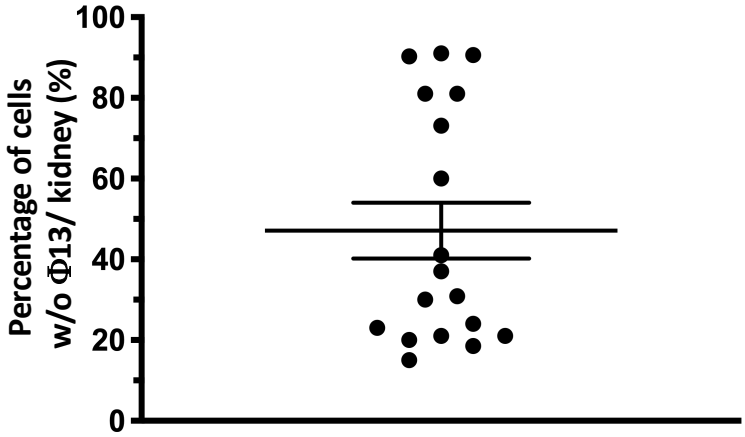
Percentage of cells w/o Φ13/ kidney (%)
100
80
60
40
20
0

Figure 2

A.

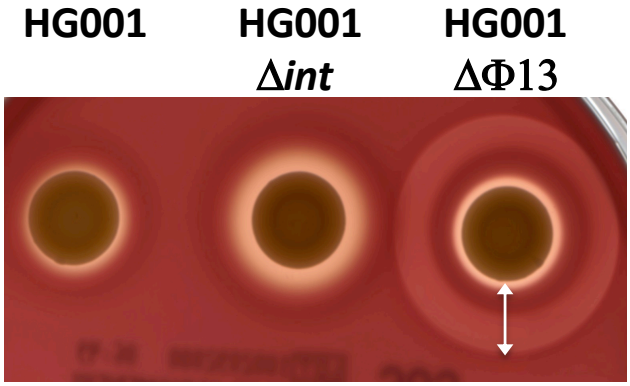
HG001
HG001
Δint
HG001
ΔΦ13

B.

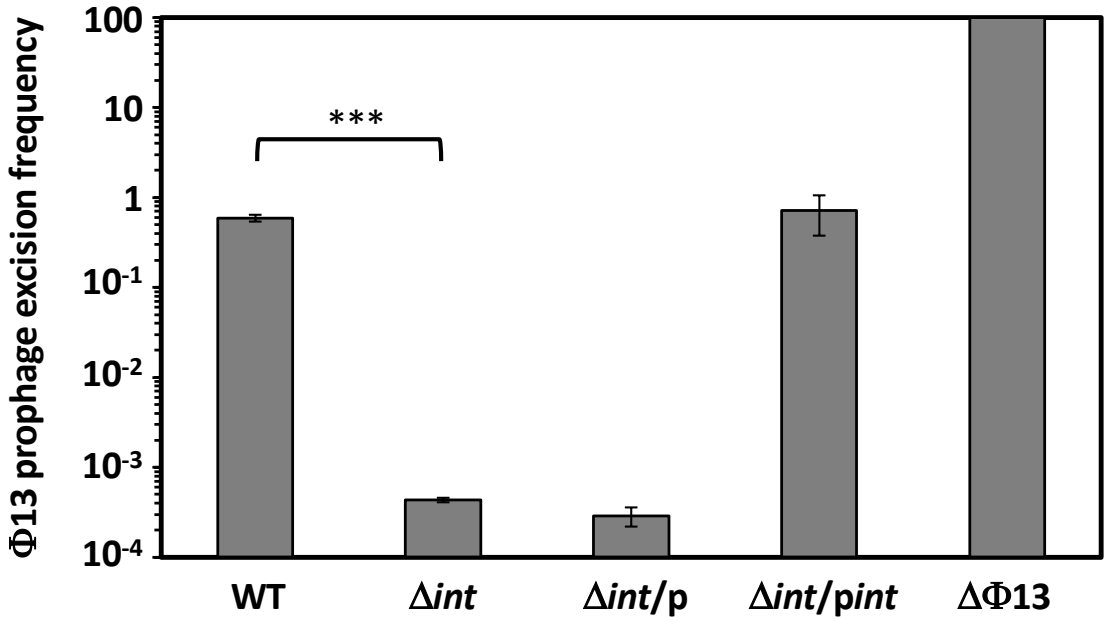
Φ13 prophage excision frequency
100
10
1
10-1
10-2
10-3
10-4
***
WT
Δint
Δint/p
Δint/pint
ΔΦ13

Figure 3

A.

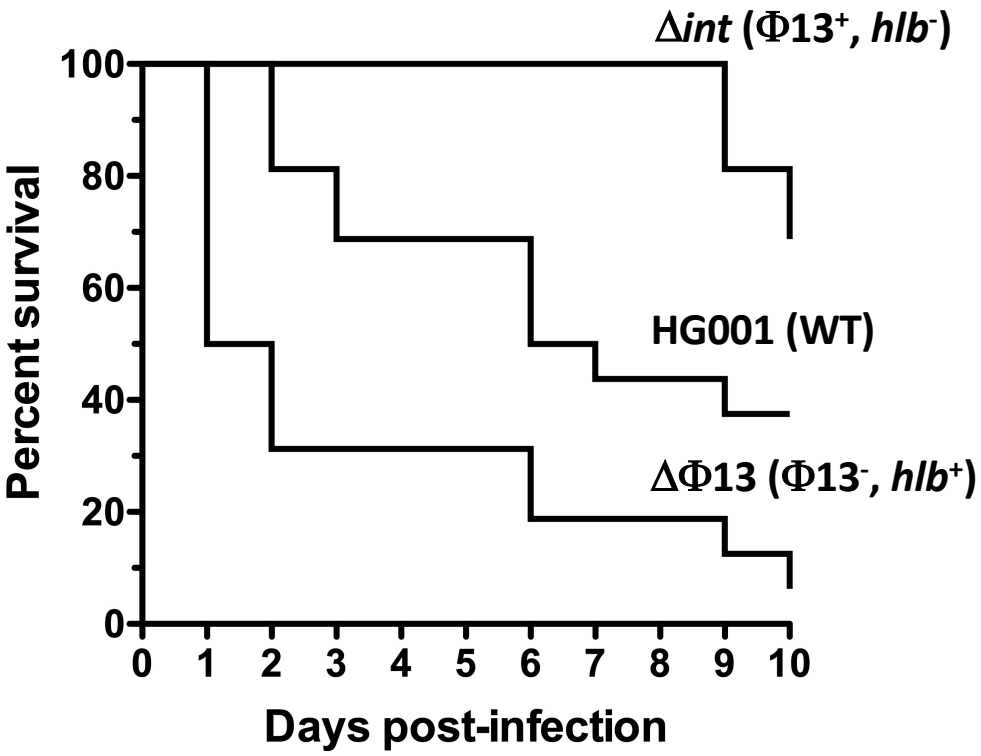
Δint (Φ13+, hlb-)
HG001 (WT)
ΔΦ13 (Φ13-, hlb+)
Percent survival
100
80
60
40
20
0
0 1 2 3 4 5 6 7 8 9 10
Days post-infection

B.

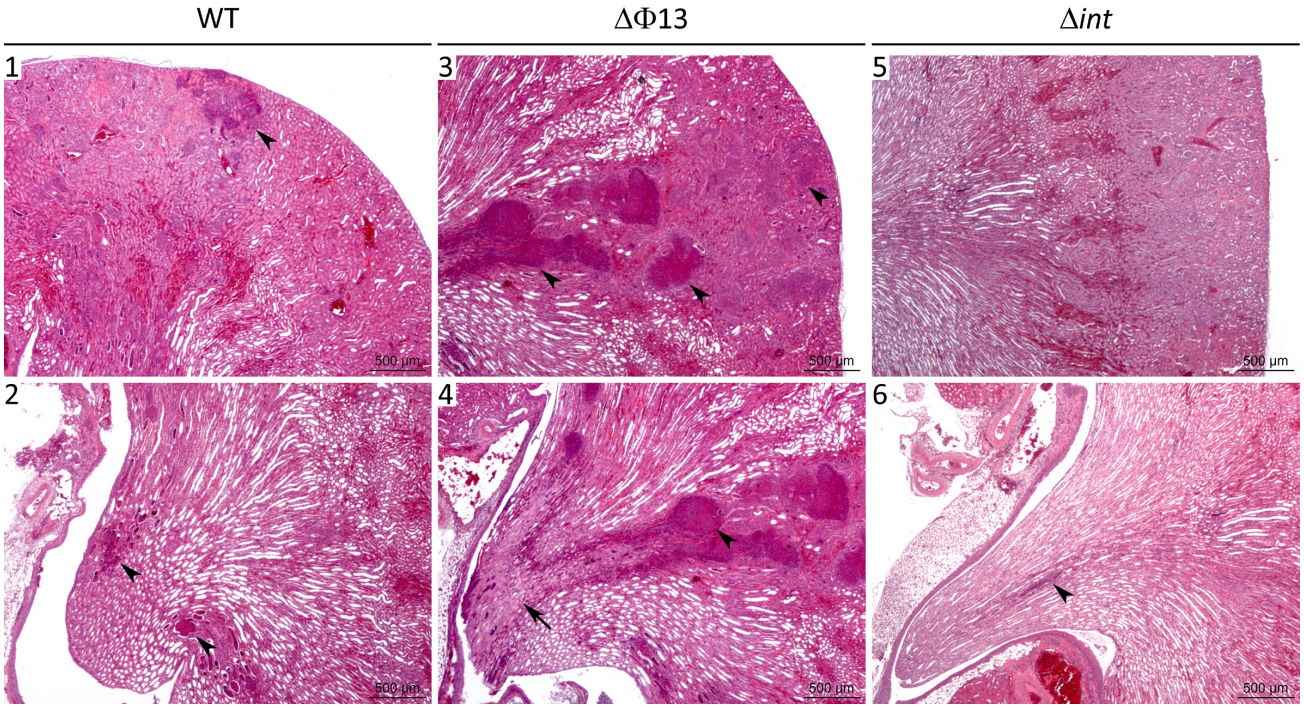
WT
ΔΦ13
Δint
1
2
3
4
5
6
500 µm

Figure 4

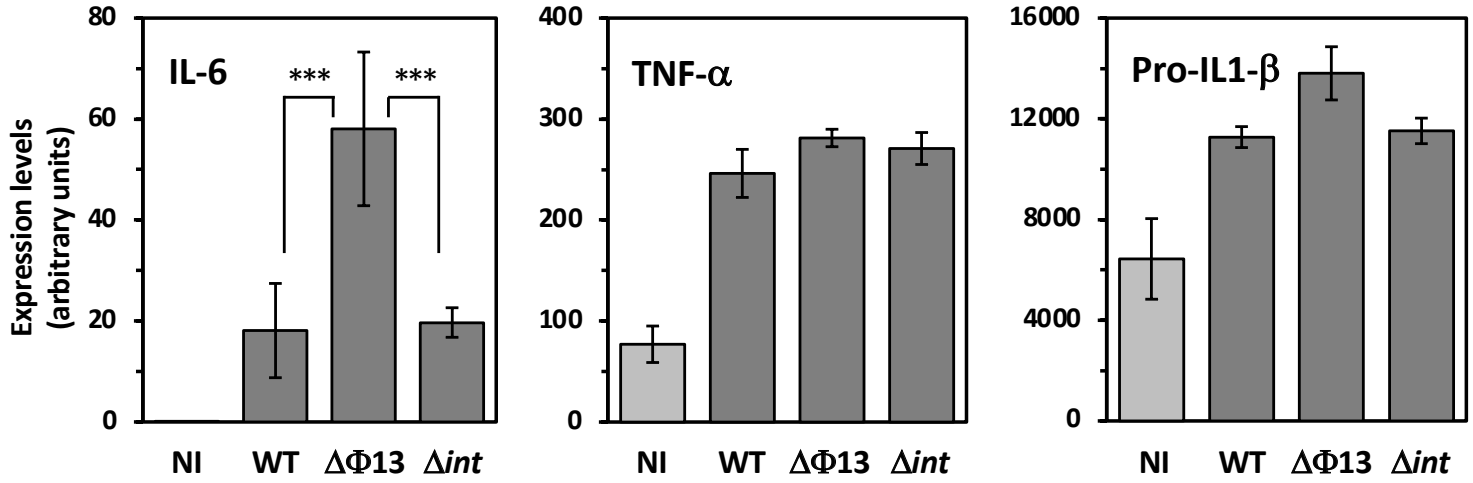
Expression levels (arbitrary units)
IL-6
***
***
80
60
40
20
0
NI
WT
ΔΦ13
Δint
TNF-α
400
300
200
100
0
NI
WT
ΔΦ13
Δint
Pro-IL1-β
16000
12000
8000
4000
0
NI
WT
ΔΦ13
Δint

Figure 5

A.

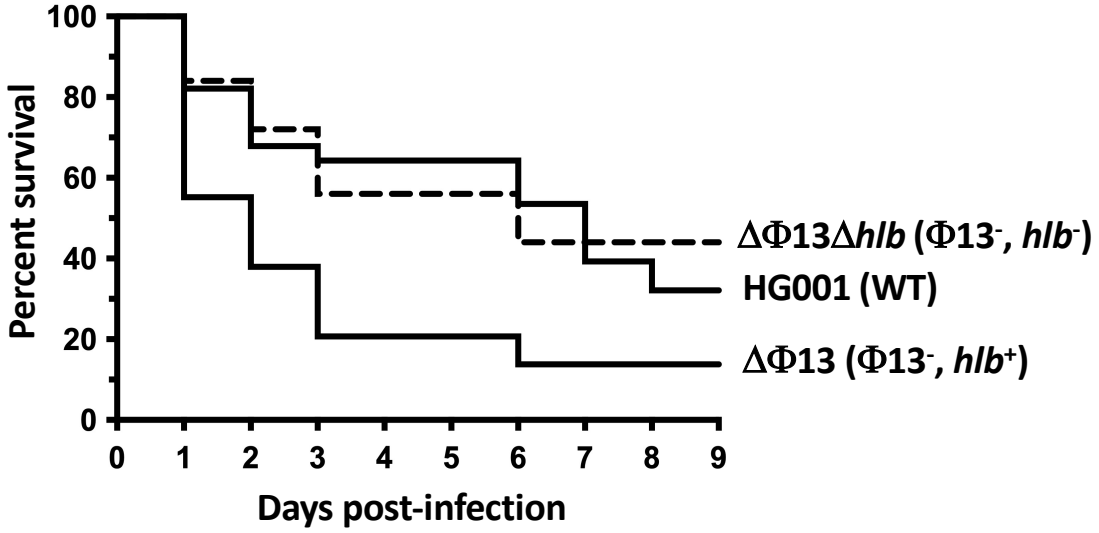
100
80
60
40
20
0
Percent survival
0 1 2 3 4 5 6 7 8 9
Days post-infection
ΔΦ13Δhlb (Φ13-, hlb-)
HG001 (WT)
ΔΦ13 (Φ13-, hlb+)

B.

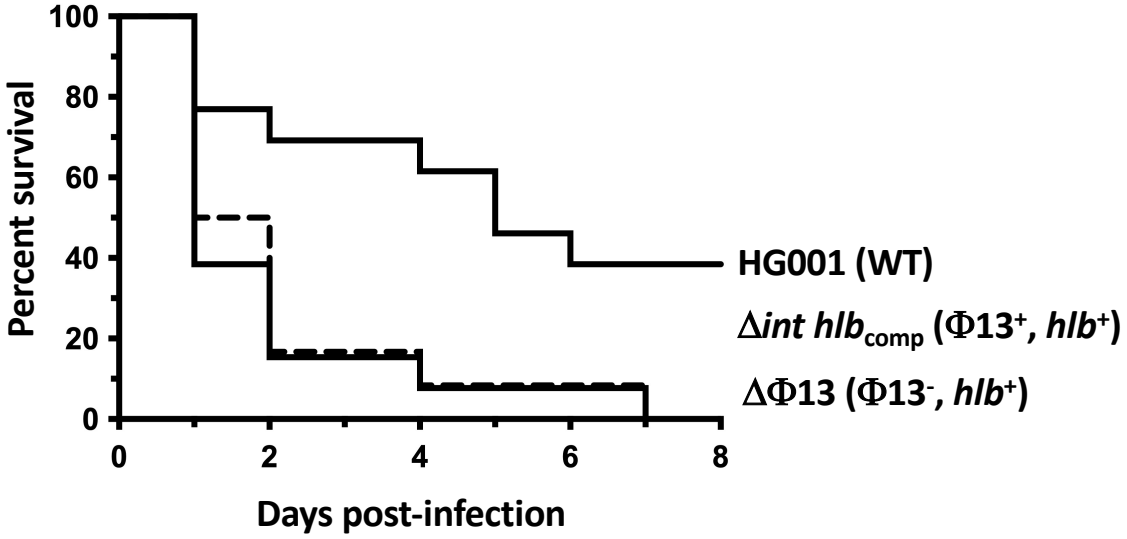
100
80
60
40
20
0
Percent survival
0 2 4 6 8
Days post-infection
HG001 (WT)
Δint hlbcomp (Φ13+, hlb+)
ΔΦ13 (Φ13-, hlb+)